ANL/ET/CP-97352

ARGONNE NATIONAL LABORATORY
9700 South Cass Avenue, Argonne, Illinois 60439

Experimental and Calculated Swelling Behavior of U-10 wt.% Mo Under Low Irradiation Temperatures*

J. Rest and G. L. Hofman ED
Argonne National Laboratory
U.S.A

and

I. Konovalov and A. Maslov
Bochvar Institute
Russia

August, 1998

*Work supported by U.S. Department of Energy, Office of Arms Control and Nonproliferation, under Contract W-31-109-Eng-38.

To be presented at the 21st International Meeting on Reduced Enrichment for Research and Test Reactors, San Paulo, Brazil, October 18-23, 1998

DISCLAIMER

Experimental and Calculated Swelling Behavior of U-10 wt.% Mo Under Low Irradiation Temperatures

J. Rest and G. L. Hofman, Argonne National Laboratory, 9700 S. Cass Ave., Argonne, IL 60439, USA

I. I. Konovalov and A. A. Maslov, Bochvar Institute, Rogov St. 5, 123060 Moscow, Russia

ABSTRACT

SEM micrographs of U-10 wt.% Mo irradiated at low temperature in the ATR to about 40 at. % burnup show the presence of cavities. We have used a rate-theory-based model to investigate the nucleation and growth of cavities during low-temperature irradiation of uranium-molybdenum alloys in the presence of irradiation-induced interstitial-loop formation and growth. In addition, the evolution of forest dislocations was calculated based on dislocation loop growth and simultaneous climb and glide of unfaulted loops. Consolidation of the dislocation structure takes into account capture of interstitial dislocation loops and annihilation of adjacent dislocations, as well as loss to grain boundaries. A di-interstitial is assumed to be the nucleus of a dislocation loop. Cavities are nucleated when two gas atoms come together in the presence of at least one vacancy. Cavity growth occurs by the influx of gas atoms and/or vacancies. In turn, the free interstitial concentration, and thus (due to recombination) the free-vacancy concentration, depends on the dislocation density. Bias-driven growth of cavities can lead to substantial swelling of the alloy (void swelling). However, our calculations indicate that the swelling mechanism in the U-10 wt.% Mo alloy at low irradiation temperatures is fission gas driven. The calculations also indicate that the observed bubbles must be associated with a sub-grain structure. Calculated swelling and bubble-size-distribution are compared with irradiation data.

INTRODUCTION

An important aspect of modeling the behavior of candidate LEU high-density uranium-alloy dispersion fuels is the identification of key irradiation-induced swelling mechanisms. The delineation of these physical processes facilitates the design of an optimal fuel type, and provides confidence in irradiation performance in regions beyond those explored experimentally. Pure uranium and various alloys of uranium that exist in the orthorhombic α-phase (e.g., U-Zr-Nb) are poor performers under irradiation due to anisotropic growth that induces grain-boundary tearing and resultant breakaway swelling. U-10 wt.% Mo is one in a series of alloys designed to maintain uranium in a metastable

cubic γ phase. The "hope" for these γ stabilized alloys is stable swelling behavior throughout fuel lifetime.

Previous calculation [1] of the irradiation-induced swelling of U-10 wt.% Mo has shown that the predicted swelling is a strong function of the steady-state value of the dislocation density. Increasing the dislocation density by a factor of two can mean the difference between gas-driven growth and bias-driven (void) growth. The bias-driven (void) growth mechanism results in significantly more swelling than the bubble driven component, and can lead to breakaway swelling behavior. Thus, it is important to pin down the dislocation kinetics. In the past both the U.S. and the Russian authors have partitioned the swelling calculations into various stages, e.g., dislocation nucleation and growth, void nucleation and growth, gas-bubble growth. However, this approach precludes the possibility that the bubble/void nucleation mechanism competes with the dislocation nucleation/growth mechanism for irradiation produced defects (vacancies and interstitials). In addition, previous calculations of the dislocation density (taken as the interstitial loop line length) have resulted in an over prediction due to ignored constraints on the growth of the loop size distribution. The loops evolve until the spacing between loops reaches a distance characteristic of that separating crystalline defects such as dislocations, grains, pores, bubbles and inclusions of a second phase. In this case we may expect the transition from a fine dislocation loop structure to a coarse dislocation forest. In what follows, a coupled model for the calculation of the dislocation density and cavity-size distribution in U-10 wt.% Mo is presented that remedies these shortcomings.

MATRIX SWELLING MODEL

The model consists of a set of coupled equations for the time rate of change of the vacancy (c_v) and interstitial (c_i) concentrations, the interstitial loop diameter (D_l) and density (N_l), the density of forest dislocation (f_d), the cavity radius (r_c) and density (c_c), the average number of gas atoms in each cavity (N_g), and, the concentration of gas atoms in solution in the fuel matrix (c_g). These equations are given by

$$\frac{dc_v(t)}{dt} = K - \alpha_r c_v c_i - k_v(\rho_l) D_v c_v, \tag{1}$$

$$\frac{dc_i(t)}{dt} = K - \alpha_r c_v c_i - k_i(\rho_l) D_i c_i - 16\pi D_i c_i c_i / a^2, \tag{2}$$

$$\frac{dN_l}{dt} = 16\pi D_i c_i c_i / (\Omega a^2) - \pi v_l(t) N_l / D_d, \tag{3}$$

$$\frac{dD_d(t)}{dt} = \frac{2}{a} v_l(t), \tag{4}$$

$$\frac{df_d}{dt} = \pi v_l(t) N_l - \sqrt{\pi} v_l(t) f_d^{3/2} - 4 v_l(t) f_d / d_g, \tag{5}$$

$$\frac{dr_c}{dt} = k_v D_v (c_v - c_v^0) - k_i D_i c_i, \tag{6}$$

$$\frac{dc_g}{dt} = G - 16\pi f_n r_g D_g c_g c_g - 4\pi r_c D_g c_c c_g + b N_g c_c, \tag{7}$$

$$\frac{dc_c}{dt} = 16\pi f_n r_g D_g c_g c_g / N_g - 16\pi D_c c_c c_c, \tag{8}$$

$$\frac{dN_g}{dt} = 4\pi r_c D_g c_g - b N_g + 16\pi N_g r_c D_c c_c, \tag{9}$$

where

$$c_v^0 = c_v^t e^{-(P_g - 2\gamma / r_c - \sigma)/\Omega kT}, \tag{10}$$

$$v_l(t) = z_i \rho_l(t) D_i c_i - z_v \rho_l(t) D_v c_v, \tag{11}$$

and

$$\rho_l(t) = \pi N_l D_l. \tag{12}$$

In the above equations, K is the damage rate in dpa/s; α_r is the usual recombination coefficient; a and Ω are the lattice constant and atomic volume, respectively; D_v, D_i, and D_g are the vacancy, interstitial, and gas-atom diffusivity, respectively; $k_v(\rho_l)$ and $k_i(\rho_l)$ are the vacancy and interstitial sink strengths, respectively; f_n is the gas bubble nucleation factor; r_g is the gas-atom radius; G is the gas-atom generation rate in atoms/cm^3/s; D_g is the gas-atom diffusivity; z_v and z_i are the vacancy and interstitial bias factors; c_v^t is the thermal equilibrium vacancy concentration; P_g is the internal gas pressure in the cavity; σ is the external stress on the cavity; and, γ is the surface energy.

The vacancy and gas-atom diffusivities are given by

$$D_v = 0.0458 e^{-\varepsilon_{vm}/kT} + \dot{f} V^{5/3} / 15, \tag{13}$$

and

$$D_g = D_g^T + \dot{f} V^{5/3} / 15. \tag{14}$$

$\dot{f}$ is the fission rate in fissions/cm^3/s, ε_{vm} is the vacancy migration energy, and D_g^T is the thermal component of the gas-atom diffusivity ($<< \dot{f} V^{5/3}/15$ at ATR temperatures). The irradiation-enhanced diffusion component of D_v and D_g was derived based on studies of structural changes taking place in two-phase uranium-molybdenum alloys under the action of neutron irradiation [2]. This assumption is reasonable if the irradiation-induced diffusion mechanism is similar to the irradiation-induced phase mixing mechanism. The volume of thermal spikes important for vacancy diffusion, V, based on calculations of temperature-time curves in the thermal spike is estimated to be 8.2×10^{-18} cm^3 at 373 K. The irradiation component of D_v was introduced to achieve physically realistic results at low temperatures for point defect concentrations and a saturated dislocation density. The value of the gas-atom diffusion coefficient given by Eq.14 lies within the scatter of the measured diffusion coefficients in oxides, mixed oxides, carbides, and nitrides [3].

The dislocation loops evolve according to Eqs.3 and 4 until the spacing between loops reaches some characteristic distance. It is assumed here that loop nucleation and growth (Eqs.3 and 4, respectively) continues until the loops contact each other, i.e.,

$$D_l(t)\rho_l(t) = 1 . \qquad (15)$$

Eq.15 yields a similar result as that based on impurity pinning.

MATRIX SWELLING ANALYSIS

Eqs.1-15 were solved numerically for a fission rate of 1×10^{14} fissions cm^{-3} s^{-1} and a fuel temperature of 373 K. Figure 1 shows the calculated total dislocation density $\rho = \rho_l + f_d$ as a function of irradiation time for two values of the vacancy migration energy ε_{vm}. ε_{vm} is the critical parameter in the theory for these operating conditions (low temperature and high fission rate). The calculations shown in Fig. 1 indicate that the dislocation density reaches a steady state value for irradiation times greater than $\approx 6 \times 10^6$ s. This time corresponds to ≈ 7.5 at.% burnup of U-10Mo. A reduction in the value of ε_{vm} from 1.1 to 0.75 eV results in an increase in the calculated dislocation density of more than an order of magnitude (i.e., from $\approx 10^9$ to $\approx 10^{10}$ cm^{-2}). A decrease in ε_{vm} translates to higher vacancy diffusivities and a higher loss rate of vacancies to sinks such as dislocations and cavities. A decrease in the vacancy concentration causes a reduction in the recombination rate between vacancies and interstitials, and thus an increase in the interstitial concentration. A higher interstitial concentration promotes increased loop nucleation and growth and results in a higher value of the dislocation density.

Figure 2 shows the calculated swelling due to matrix cavities for the same two

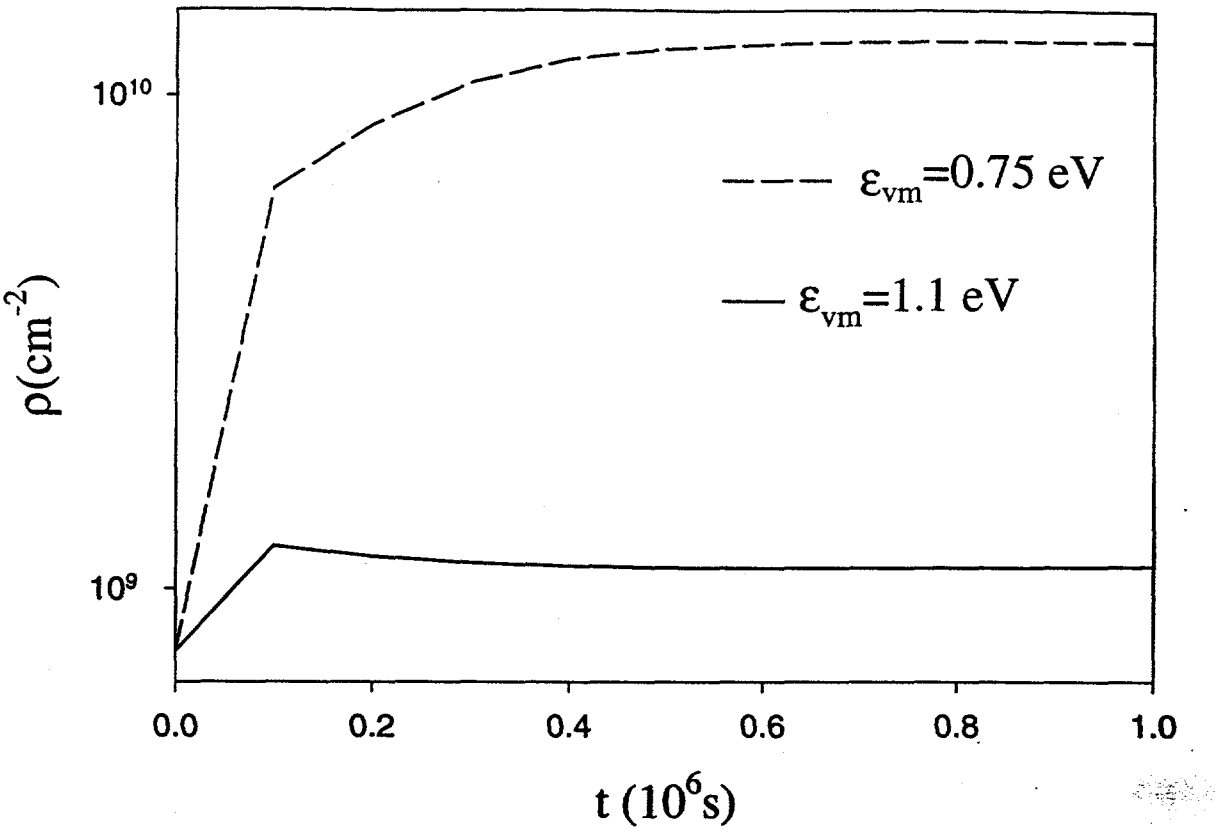

Figure 1. Calculated total dislocation density $\rho = \rho_l + f_d$ as a function of irradiation time for two values of the vacancy migration energy ε_{vm}.

values of ε_{vm}. A value for ε_{vm} of 1.1 eV results in matrix swelling << 1% for fuel-particle burnups > 40 at.%. However, a value for ε_{vm} of 0.75 eV results in cavity-induced matrix swelling > 200%! The reason for this dramatic four order of magnitude increase in swelling for a 25% decrease in vacancy migration energy has its roots in the difference between gas-driven (gas bubble) and bias-driven (void) swelling mechanisms.

In order to understand the nature of cavity swelling in the material, it is instructive to examine the behavior of the excess cavity pressure $P_g - 2\gamma / r_c$ that appears in the exponent in Eq.10 (in the following, the value of the external pressure σ is assumed to be negligible). Fig. 3 shows the calculated excess cavity pressure for the two values of ε_{vm} as a function of irradiation time. As shown in Fig. 3, for ε_{vm} = 1.1 eV

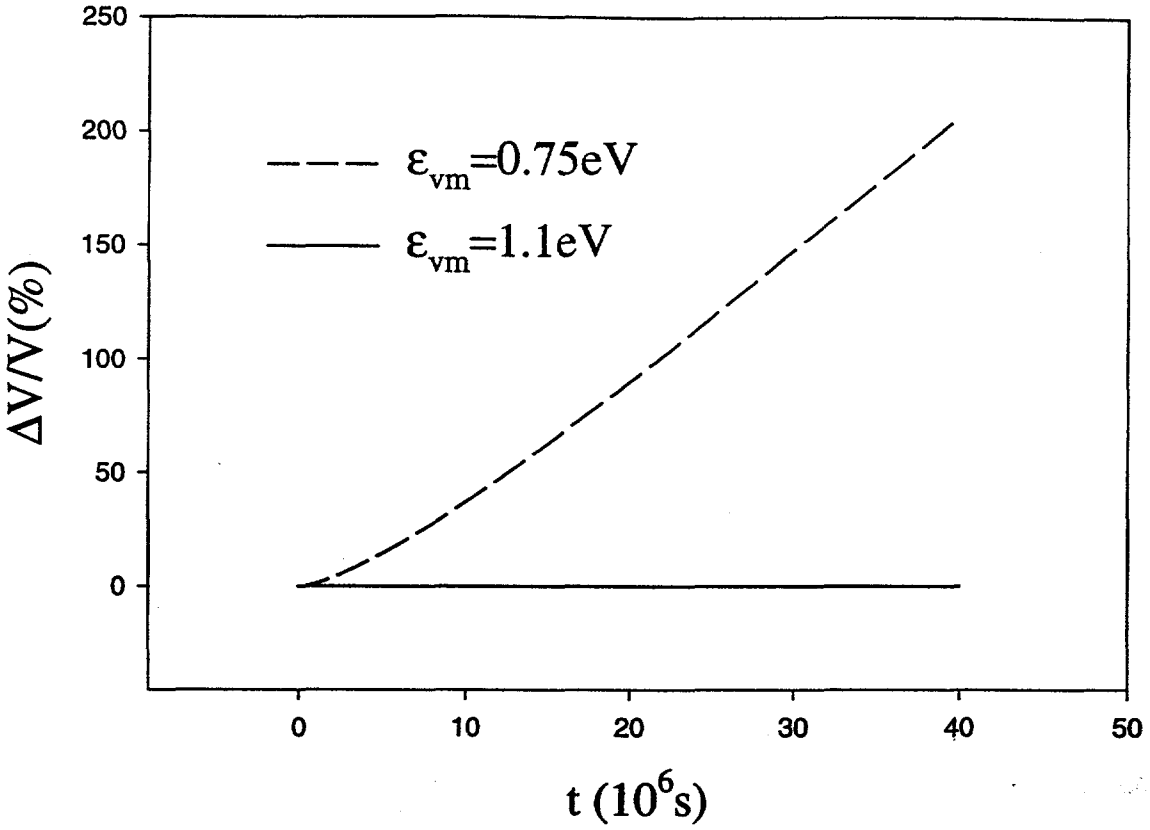

Figure 2. Calculated swelling due to matrix cavities for two values of ε_{vm}

$P_g - 2\gamma / r_c$ is positive and increasing throughout the irradiation period. This means that the gas pressure within the cavity, P_g, is greater than the surface tension, $2\gamma / r$, and the cavity is behaving like a gas bubble. The excess cavity pressure increases because of an insufficient number of available vacancies in the matrix required for equilibration. If sufficient vacancies are made available (e.g., by creep processes), bubble growth will continue until the bubbles become equilibrated (excess pressure equal to zero). Continued bubble growth requires the diffusion of gas atoms as well as vacancies to the bubble. Bubble growth is also limited due to irradiation-induced gas-atom re-solution from bubbles. For these reasons, swelling due to bubble growth is generally well behaved (linear).

On the other hand, as shown in Fig. 3, for $\varepsilon_{vm} = 0.75$ eV the excess pressure is negative throughout the entire irradiation period. For this case, the surface tension is greater than the internal gas pressure, and, as the right hand side of Eq.6 is positive due to

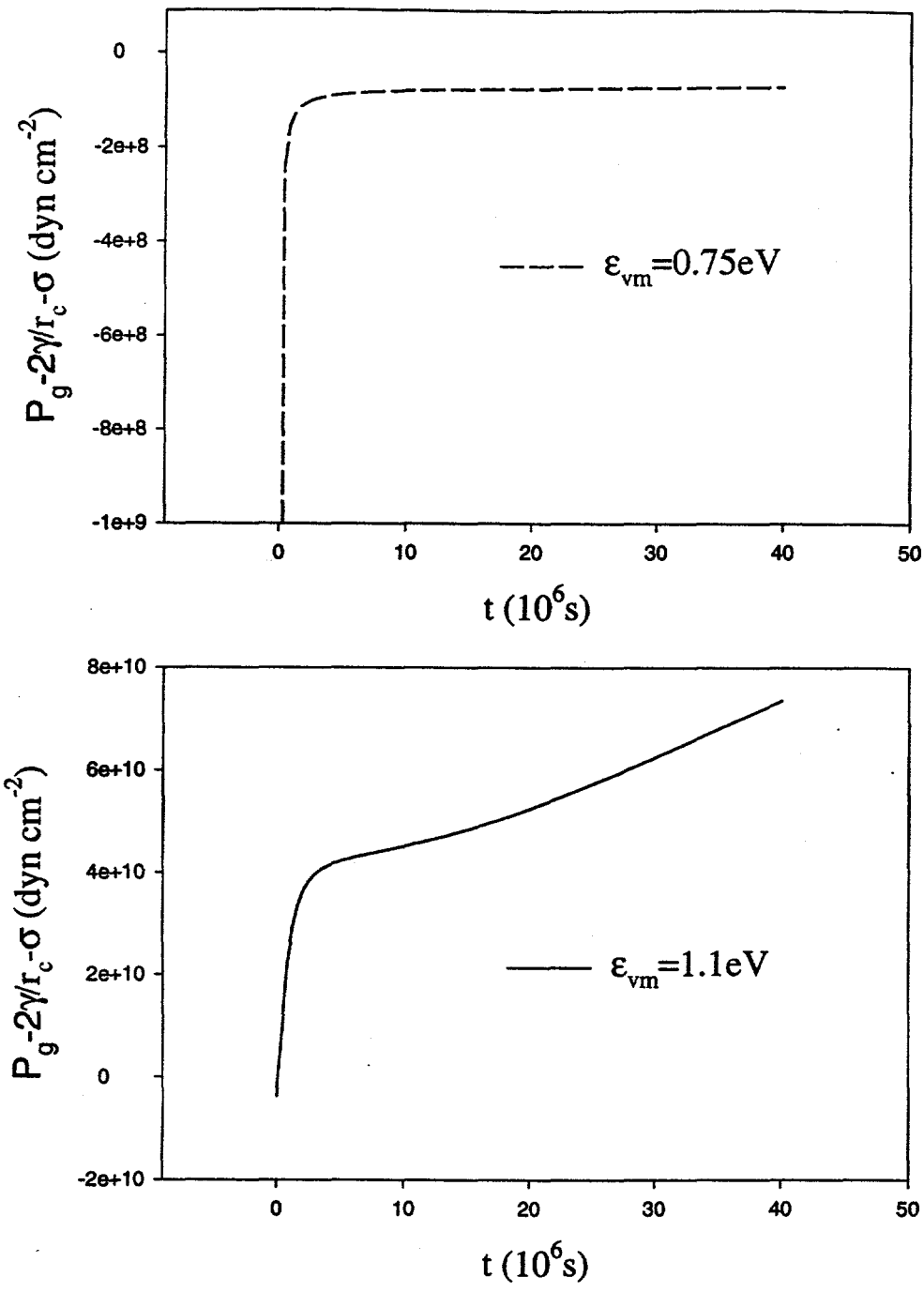

Fig.3. Calculated excess cavity pressure for two values of ε_{vm} as a function of irradiation time.

a super saturation of vacancies in the lattice, the cavity grows by the influx of vacancies. Continued cavity growth under these conditions (bias-driven void growth) requires only

excess vacancies in the lattice. For this reason, void growth can lead to unstable swelling behavior.

A key question is whether the irradiation-induced swelling of U-10Mo is bubble or biased driven. If bubble driven, the swelling is expected to be stable. If biased driven, the swelling could become unstable at high burnup leading to unacceptable materials behavior during irradiation. Given the above analysis, this question can be rephrased as to whether the vacancy migration energy in U-10Mo is closer to 1.1 eV or to 0.75 eV.

There is an observed linear relationship between the activation energy of uranium self-diffusion in body-centered cubic metals and the melting point of the metals under consideration [4]. This relationship can be expressed as

$$Q_{self} = kT_{melt}, \tag{16}$$

$$k = 1.453\text{x}10^{-3}\,\text{eV}/(\text{at K}).$$

The energy for self-diffusion, Q_{self}, is related to the vacancy migration, ε_{vm}, and formation, ε_{vf}, energies by

$$Q_{self} = \varepsilon_{vm} + \varepsilon_{vf}. \tag{17}$$

In general, $\varepsilon_{vm} \approx 0.5 Q_{self}$ so that

$$\varepsilon_{vm} = 7.265x10^{-4} T_{melt}\ (\text{eV/K}). \tag{18}$$

For metastable alloys, such as U-10 wt.% Mo, the assumption is made that the solidus point represents the melting point. For U-10 wt.% Mo the solidus occurs at 1520K. Thus, from Eq.18, $\varepsilon_{vm} = 1.1$ eV. Thus, from the analysis illustrated by Figs.1-3, we are forced to the conclusion that any cavities in the lattice of the irradiated U-10 wt.% Mo are gas bubbles and not voids.

GRAIN-BOUNDARY SWELLING ANALYSIS

Irradiation-induced recrystallization and enhanced bubble growth on the newly formed grain boundaries was proposed as an interpretation of the observed fission-gas-bubble-size distribution and swelling curve for U_3Si_2 aluminum dispersion fuels and for UO_2 power reactor fuels [5]. Recrystallization and intergranular bubble growth has been definitively confirmed for UO_2 fuels [6]. Based on this experience, it was natural for the authors to suppose that cavities, if observed, should be associated with a sub-grain structure.

Figure 4 shows DART [7] calculated fission-gas-bubble-size distributions for U-10 wt.% Mo irradiated in the ATR at ≈40 at.% burnup for two recrystallization scenarios.

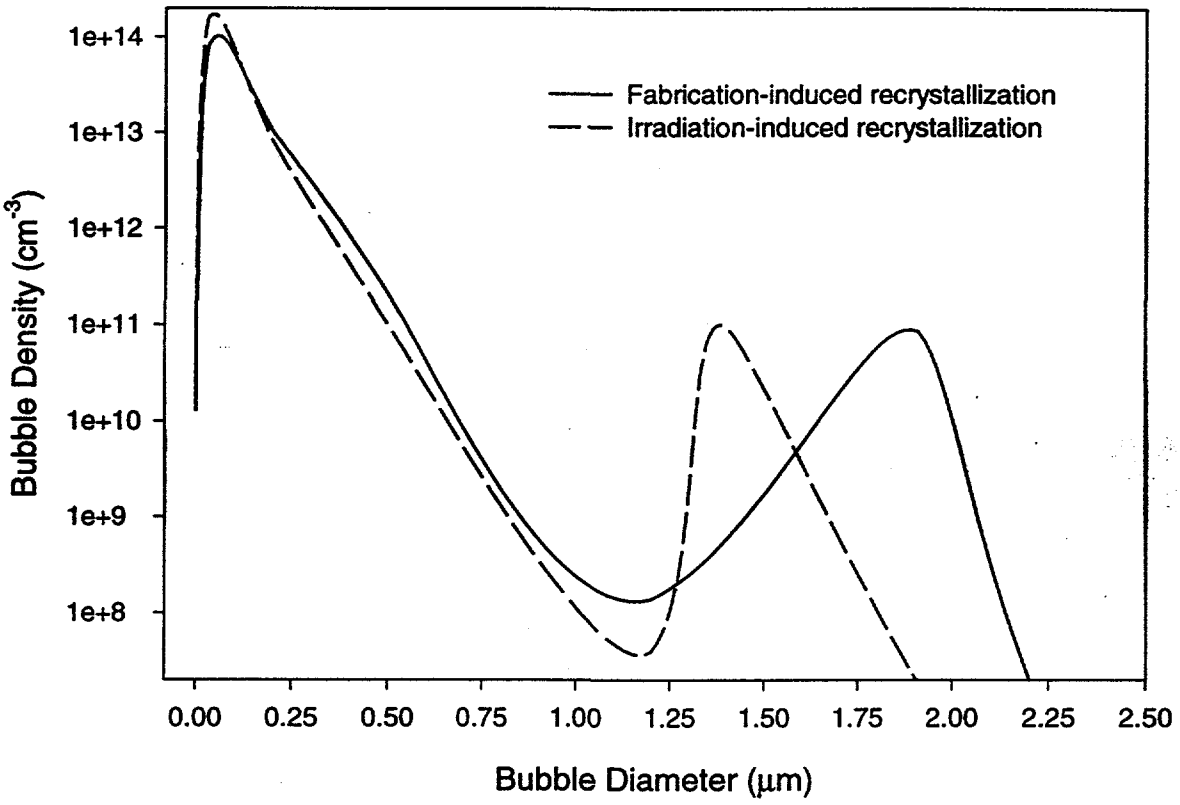

Fig.4. DART calculated fission-gas-bubble-size distributions for U-10 wt.% Mo irradiated in the ATR to ≈40 at.% burnup for two recrystallization scenarios

The scenario represented by the solid line in Fig.4 is recrystallization induced in the heavily deformed fuel particles due to grinding during fuel fabrication at ≈ 500°C. For this case 2μm size grains are presumed to have formed during fabrication and are assumed to exist in the fuel during the entire irradiation. The scenario represented by the dashed line in Fig.4 is irradiation-induced recrystallization. The DART recrystallization model developed for U_3Si_2 fuels was utilized for this case. The model predicts that

recrystallization occurs at a fuel-particle fission density of 2.6×10^{21} cm^{-3} ($\approx$33 at.% burnup). Again, the recrystallized grain size is assumed to be 2μm. For both scenarios, the calculated peaks of the bimodal distributions are associated with grain boundary (larger peak) and grain corner (smaller peak) bubbles. The calculated intragranular bubble sizes are well below those resolvable experimentally by scanning electron microscopy. The calculations shown in Fig.4 predict that the larger bubble peak will occur at a smaller bubble size for the case of irradiation-induced recrystallization than for the case of fabrication-induced recrystallization. This is because for irradiation-induced recrystallization the time that bubbles have to accumulate and grow on the grain boundaries is shorter than for fabrication-induced recrystallization.

Fig.5 shows an SEM micrograph of U-10 wt.% Mo fabricated from ground powder irradiated in the ATR to $\approx$40 at.% LEU burnup. Recrystallized grains with diameter $\approx$ 2 μm and gas bubbles associated with the grain surfaces are clearly seen in the micrograph. The bubbles appear to form a bimodal distribution with the larger diameter (smaller density) population having sizes $\approx$1-1.5 μm. Measured bubble-size distributions are currently not available. However, it is clear that the calculated distributions as shown in Fig. 4 are in qualitative agreement with the observed bubbles shown in Fig. 5.

Fig.6 shows the calculated fuel-particle swelling as a function of particle fission density. 40 at.% burnup occurs at $\approx 3.1 \times 10^{27}$ m^{-3}. The difference between the fission-gas-bubble swelling (dashed curve) and the total fission-product swelling (solid) curve is the solid-fission product swelling contribution. Swelling due to the interaction between the fuel particle and the aluminum matrix has not been included in Fig.6. As can be seen from the results shown in Fig.6, the swelling is linear throughout the entire irradiation period. The total calculated fission-product swelling at $\approx$80 at.% burnup is $\approx$100%. This swelling behavior is similar to that observed for U_3Si_2

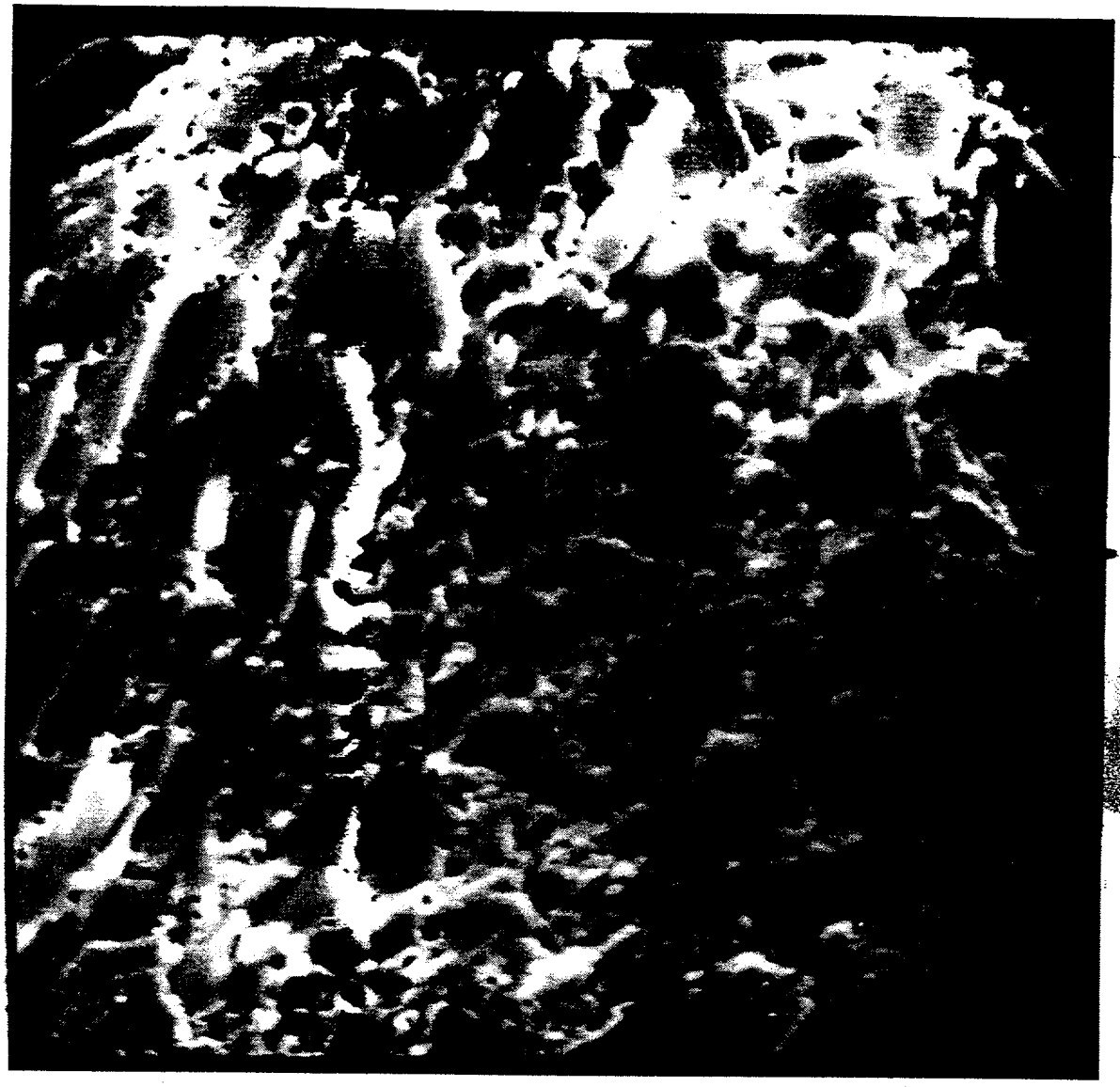

Fig.5. SEM micrograph of U-10 wt.% Mo fabricated from ground powder irradiated in the ATR to ≈40 at. % LEU burnup

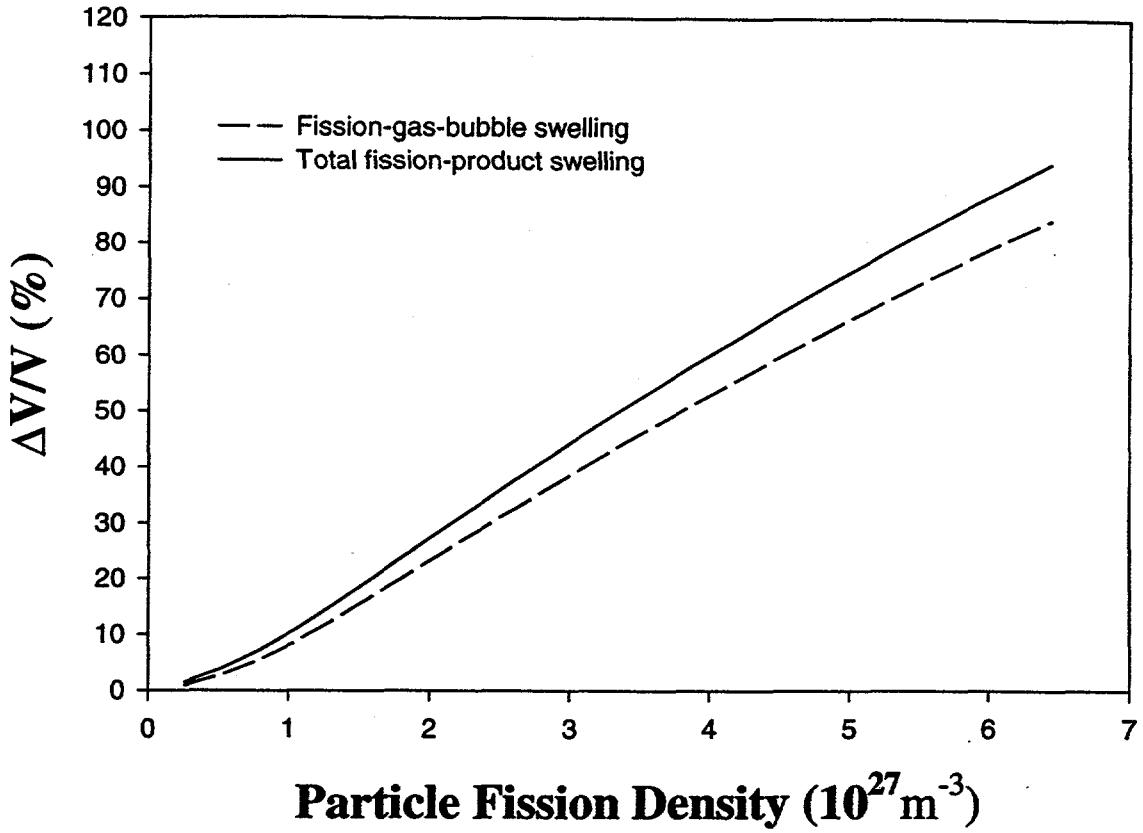

Fig.6. Calculated fuel-particle swelling as a function of particle fission density

CONCLUSIONS

SEM micrographs of U-10 wt.% Mo irradiated at low temperature in the ATR to about 40 at. % burnup show the presence of cavities. We have used a rate-theory-based model to investigate the nucleation and growth of cavities during low-temperature irradiation of uranium-molybdenum alloys in the presence of irradiation-induced interstitial-loop formation and growth. In addition, the evolution of forest dislocations was calculated based on dislocation loop growth and simultaneous climb and glide of unfaulted loops. Consolidation of the dislocation structure takes into account capture of interstitial dislocation loops and annihilation of adjacent dislocations, as well as loss to grain boundaries. Bias-driven growth of cavities can lead to substantial swelling of the alloy (void swelling). However, our calculations indicate that the swelling mechanism in the U-10 wt.% Mo alloy at low irradiation temperatures is fission gas driven. The calculations also indicate that the observed bubbles must be associated with a sub-grain structure. Calculated swelling and bubble-size-distribution are in qualitative agreement with the observations. The model predicts that U-10 wt.% Mo will exhibit stable fission-product-swelling behavior throughout its lifetime.

REFERENCES

1. J. Rest, G. L. Hofman, K. L. Coffey, I. Konovalov and A. Maslov, "ANALYSIS OF THE SWELLING BEHAVIOR OF U-ALLOYS," To be published in the proceedings of the 20th International Meeting on Reduced Enrichment for Research and Test Reactors, Jackson Hole, WY., October 5-11, 1997.

2. S. T. Konobeevsky, K. P. Dubrovin, B. M. Levitsky, L. D. Panteleev, and N. F. Pravdyuk, Second Geneva Conference paper 232, 1958.

3. Hj. Matzke, in Diffusion Processes in Nuclear Materials, R.P. Agarwala, editor, Elsevier Science Publishers B.V. (1992) 9-69

4. G. B. Fedorov and E. A. Smirnov, "Diffusion in Reactor Materials," Published for the National Bureau of Standards, United States Department of Commerce and the National Science Foundation, Washington, D.C., by Amerind Publishing Co. Pvt. Ltd., New Delhi, India (1984)

5. J. Rest and G. L. Hofman, J. Nucl. Mater., 210 (1994) 187-202.

6. K. Nogita and K. Une, Nucl. Instr. And Meth. B 91 (1994) 301.

7. J. Rest, "The DART Dispersion Analysis Research Tool: A Mechanistic Model for Predicting Fission-Product-Induced Swelling of Aluminum Dispersion Fuels," ANL-95/36, Argonne National Laboratory (August, 1995).